

A Noncausal Linear Prediction Based Switching Median Filter for the Removal of Salt and Pepper Noise

B. Deka and D. Baishnab

Department of Electronics and Communication Engineering

Tezpur Central University

Tezpur, 784028, India

Email: bdeka@tezu.ernet.in, baishnabd@gmail.com

Abstract—In this paper, we propose a switching based median filter for the removal of impulse noise, namely, the salt and pepper noise in gray scale images. The filter is based on the concept of substitution of noisy pixels prior to estimation. It effectively suppresses the impulse noise in two stages. First, the noisy pixels are detected by using the signal dependent rank-ordered mean (SD-ROM) filter. In the second stage, the noisy pixels are first substituted by the first order 2D noncausal linear prediction technique and subsequently replaced by the median value. Extensive simulations are carried out to validate the proposed method. Experimental results show improvements both visually and quantitatively compared to other switching based median filters for the removal of salt-and-pepper noise at different densities.

Index Terms—Impulse noise, Detection based median filter, Noncausal linear prediction

I. INTRODUCTION

Digital images are frequently corrupted by impulse noise during the process of image acquisition and/or transmission. Preserving the image details and attenuation of noise are the two important aspects of image processing which are always contradictory in nature. So the research emphasis is on the removal of impulse noise while keeping the loss of details to minimum. There are two types of impulse noises, namely, the salt-and-pepper noise and the random valued impulse noise.

Linear filtering techniques do not perform well for the removal of impulse noise. On the other hand, nonlinear techniques have been found superior and provide more satisfactory results while preserving image details. The most basic nonlinear filter is the standard median (SM) filter [1]. The SM filter works effectively at low noise densities but at the cost of blurring the image. One way to improve this situation is to use the weighted median (WM) filter [2] which gives more weight to some values within the window than others. The special case of the WM filter is the center weighted median (CWM) [3] filter which gives more weight only to the center value of the window. The major drawback of these filters is that they do not detect *a priori* whether a pixel in the image is actually corrupted by impulse or not and simply replaces every pixel by the median value of the pixels in its fixed neighborhood. A better strategy to circumvent this drawback is to incorporate some decision-making processes

or switching in the filtering framework.

The switching based median filter performs well for the removal of impulse noise in comparison to the CWM filter with better preservation of details. Some of the state-of-the-art switching based median filters are the rank-conditioned mean (RCM) [4], the signal-dependent rank ordered mean (SDROM) [5], the tri-state median (TSM) [6] filter, the adaptive center weighted median (ACWM) [7] filter, the directional weighted median (DWM) [8], the adaptive switching median (ASWM) [9], and the new switching based median (NSWM) [10] filters. In the SD-ROM filter, multiple thresholds are considered in detection of the corrupted pixels and then the detected pixels are replaced by the rank-ordered mean (ROM) value of the pixels in the current window. Another recently proposed switching based median filter with preservation of fine details on images corrupted by the salt and pepper noise is the *new switching based median* (NSWM) filter. This filter uses the concept of substitution of noisy pixels prior to estimation. It employs the causal 1D linear prediction strategy for the substitution of *all* the noisy pixels within a window.

The NSWM filter has been found to perform quite well for the removal of salt and pepper noise at high noise ratios [10]. However, it does not utilize the 2D structure of an image for the prediction of the noisy pixels and hence does not exploit the interline dependence of the pixels in an image. Therefore, the performance of the NSWM filter may be further improved by considering the natural structure of the pixels in an image. Moreover, it applies a very simple technique for the detection of the noisy pixels. In this filter any pixel having a value of either 0 or 255 are considered as the noisy pixels. However, in practice this may not be always true. In fact, the uncorrupted image may also have some pixels of values of either 0 or 255, so there is probability that some of the uncorrupted pixels in the image might also falsely get detected as the noisy pixels.

In this paper, we propose a two stage switching based median filter for the removal of salt and pepper noise from gray scale images. In the first stage, the noisy pixels are detected by the detection stage of the SD-ROM filter. In the second stage, if a pixel is detected to be noisy then it is first substituted by using the 2D noncausal linear prediction from the neighboring pixels in a window centered at this pixel and subsequently the pixel is estimated from the predicted pixel

and its neighbors by computing the median. The uncorrupted pixels in the image are left unchanged. Finally, experiments are carried out to evaluate the proposed method both visually and quantitatively. The rest of the paper is organized as follows. In Section II, we review the impulse noise detection using the SD-ROM filter. Section III gives a brief overview of the 2D non causal linear prediction in gray scale images. The proposed switching median filter is discussed in Section IV. Section V gives the simulation results using different test images. Finally, conclusions are drawn in Section VI.

II. REVIEW OF THE SD-ROM FILTER

Consider an 8-bit gray scale image \mathbf{X} . Let $Y(i, j)$ be the gray value of the noisy image \mathbf{Y} at pixel (i, j) and $W(i, j)$ be a window centered at (i, j) . We assume here the following impulse noise model:

$$Y(i, j) = \begin{cases} X(i, j), & \text{with probability } 1 - \gamma \\ R(i, j), & \text{with probability } \gamma \end{cases}, \quad (1)$$

where $X(i, j)$ and $R(i, j)$ denote the pixel values at location (i, j) in the original image and the noisy image, respectively and γ is the noise ratio/density. In an 8-bit gray scale image, the salt and pepper noise $R(i, j)$ can take either 0 or 255. Since the proposed scheme uses the impulse detection stage of the SD-ROM filter, a brief review of this filter is given below.

The SD-ROM filter consists of the following two stages [5]:

A. Impulse noise detection:

- Consider a 3×3 window \mathbf{W} centered at $Y(i, j)$. Define an observation vector containing the pixels in the neighborhood of and obtained by a left-right, top-to-bottom scan of the window:

$$\mathbf{w} = [w_1, w_2, \dots, w_8]$$

- Arrange the observation vector \mathbf{w} by their ranks Δ given by $\Delta = [\Delta_1, \Delta_2, \dots, \Delta_8]$ such that $\Delta_1 \leq \Delta_2 \leq \dots \Delta_8$.
- Define the rank-ordered mean (ROM) by $M = (\Delta_4 + \Delta_5) / 2$. Obtain the rank-ordered differences τ^d , where

$$\tau_i^d = \begin{cases} \Delta_i - Y(i, j), & \text{if } Y(i, j) \leq M \\ Y(i, j) - \Delta_{9-i}, & \text{otherwise,} \end{cases} \quad (2)$$

for $i = 1, \dots, 4$.

- Consider $Y(i, j)$ to be noisy if $\tau_i^d > T_i$, where T_1, T_2, T_3 and T_4 are threshold values such that $T_i < T_{i+1}$,

for $i = 1, \dots, 4$.

B. Estimation of the true value:

$$Y(i, j) = \begin{cases} M, & \text{if } Y(i, j) \text{ noisy} \\ X(i, j), & \text{otherwise.} \end{cases} \quad (3)$$

III. NONCAUSAL LINEAR PREDICTION

In the noncausal linear prediction, a noncausal neighborhood of pixels is used to make a linear prediction of current pixel. The first-order 2D linear predicted value of the center pixel $Y(i, j)$ in a 3×3 noncausal neighborhood is given by [11]:

$$\begin{aligned} \hat{Y}(i, j) &= a_{0,1} \{Y(i, j-1) + Y(i, j+1)\} \\ &+ a_{1,0} \{Y(i-1, j) + Y(i+1, j)\} \\ &= \mathbf{Y}^T \mathbf{a}_1, \end{aligned} \quad (4)$$

$$\mathbf{Y} = [\{Y(i, j-1) + Y(i, j+1)\},$$

where

$$Y(i-1, j) + Y(i+1, j)]^T$$

considering samples at horizontal row and vertical column only in the prediction window. Here, $\mathbf{a}_1 = [a_{0,1}, a_{1,0}]^T$ represents the prediction coefficient vector. The first-order prediction coefficients are related with the autocorrelation functions by the following Wiener-Hopf equation [12]:

$$\mathbf{R}_{Y_1} \mathbf{a}_1 = \mathbf{r}_{Y_1} \quad (5)$$

The solution of the above matrix equation gives the prediction coefficient vector \mathbf{a} . Using the symmetry property $\mathbf{R}_{Y_1}(i, j) = \mathbf{R}_{Y_1}(-i, -j)$ of the autocorrelation function of wide-sense stationary image random field, it can be shown that [13]:

$$a_1(-i, -j) = a_1(i, j). \quad (6)$$

The symmetry property is used for the computation of the prediction coefficients. For first-order 2D noncausal linear prediction

$$\mathbf{R}_{Y_1} = \begin{bmatrix} R_{Y_1}(0,0) + R_{Y_1}(2,0) & 2R_{Y_1}(1,1) \\ 2R_{Y_1}(1,1) & R_{Y_1}(0,0) + R_{Y_1}(0,2) \end{bmatrix},$$

$$\text{and } \mathbf{r}_{Y_1} = \begin{bmatrix} R_{Y_1}(1,0) \\ R_{Y_1}(0,1) \end{bmatrix}.$$

For better estimation of the predicted value, the diagonal values of the 3×3 noncausal neighborhood are also considered. This leads to the second order 2D noncausal linear prediction filter which is given by

$$\hat{Y}(i, j) = \begin{bmatrix} Y(i, j-1) + Y(i, j+1) \\ Y(i-1, j) + Y(i+1, j) \\ Y(i-1, j-1) + Y(i+1, j+1) \\ Y(i-1, j+1) + Y(i+1, j-1) \end{bmatrix}^T \begin{bmatrix} a_2(0,1) \\ a_2(1,0) \\ a_2(1,1) \\ a_2(1,-1) \end{bmatrix}, \quad (7)$$

and the prediction coefficients are obtained from

$$\mathbf{R}_{Y_2} = \mathbf{a}_2 \mathbf{r}_{Y_2} \quad (8)$$

where

$$\mathbf{R}_Y = \begin{bmatrix} R_Y(0,0)+R_Y(0,2) & R_Y(1,-1)+R_Y(1,1) & R_Y(1,0)+R_Y(1,2) & R_Y(1,-2)+R_Y(1,0) \\ R_Y(1,-1)+R_Y(1,1) & R_Y(0,0)+R_Y(2,0) & R_Y(0,1)+R_Y(2,1) & R_Y(0,1)+R_Y(2,-1) \\ R_Y(1,0)+R_Y(1,2) & R_Y(0,1)+R_Y(2,1) & R_Y(0,0)+R_Y(2,2) & R_Y(0,2)+R_Y(2,0) \\ R_Y(1,-2)+R_Y(1,0) & R_Y(0,1)+R_Y(2,-1) & R_Y(0,2)+R_Y(2,0) & R_Y(0,0)+R_Y(2,-2) \end{bmatrix}$$

and

$$\mathbf{r}_{Y_2} = \begin{bmatrix} R_Y(0,1) \\ R_Y(1,0) \\ R_Y(1,1) \\ R_Y(1,-1) \end{bmatrix}$$

For numerical implementation, the autocorrelation functions in Equations (5) and (8) are replaced by the estimated autocorrelation functions. The estimated autocorrelation function, estimated from the pixels in a block of size $P \times Q$ is given by

$$\hat{R}_Y(i, j) = \frac{1}{PQ} \sum_{s=1}^{P-|i|} \sum_{t=1}^{Q-|j|} Y(s, t) Y(s+|i|, t+|j|) \quad (9)$$

IV. PROPOSED SWITCHING MEDIAN FILTER

The block diagram of the proposed filter is shown in Fig. 1. The filter is based on the concept of substitution of noisy pixels prior to estimation. It mainly consists of two stages. In the first stage, the noisy pixels are detected by the impulse

detection stage of the SD-ROM filter. We have used the SDROM filter because of its ability to detect an impulse with very good accuracy even in the presence of multiple impulses within the sliding window. It applies four distinct rank-ordered differences to detect an impulse. The rank-ordered differences are then compared with four increasing thresholds as described in Section II.

In the second stage, if a pixel is considered to be noisy, it is substituted by performing a first-order 2D noncausal linear prediction from the neighborhood pixels in the current window prior to estimation as described in Section III. Then the noisy pixel is replaced by the median value of the pixels within that window. This strategy is found to be very effective than the conventional method of replacing an impulse by the median value in the switching based median filters because here the corrupted center pixel is not directly included in the filtering window to compute the median value [10]. Instead, it is first smoothed by predicting its value from its 2D noncausal neighborhood in the image prior to estimation.

In the present development of the algorithm, we consider both the first and second order 2D noncausal linear prediction techniques in order to estimate the predicted value from the pixels in the noncausal neighborhood. The uncorrupted pixels in the image are kept unaltered.

The proposed algorithm can be summarized as follows:

Algorithm 1 Proposed Switching Median Filter

1. Input \mathbf{Y}
2. Repeat
3. Select a 3×3 window \mathbf{W} with $Y(i, j)$ being its center.
4. Apply the impulse detection stage of the SD-ROM filter described in Section II for the pixels in
5. IF is noisy, estimates prediction coefficients using Equations (5) and (8) in Section III and substitute the same to estimate using Equation (4) and (7), respectively, otherwise it is kept unaltered.
6. Arrange the pixels in with center to an 1D array.
7. Find the median value of.
8. Finally, replace by the median value of the noncausal neighborhood with as the center.
9. ELSE keep remain unchanged.
10. Until all is in \mathbf{Y} .
11. Finally, obtain the denoised image.

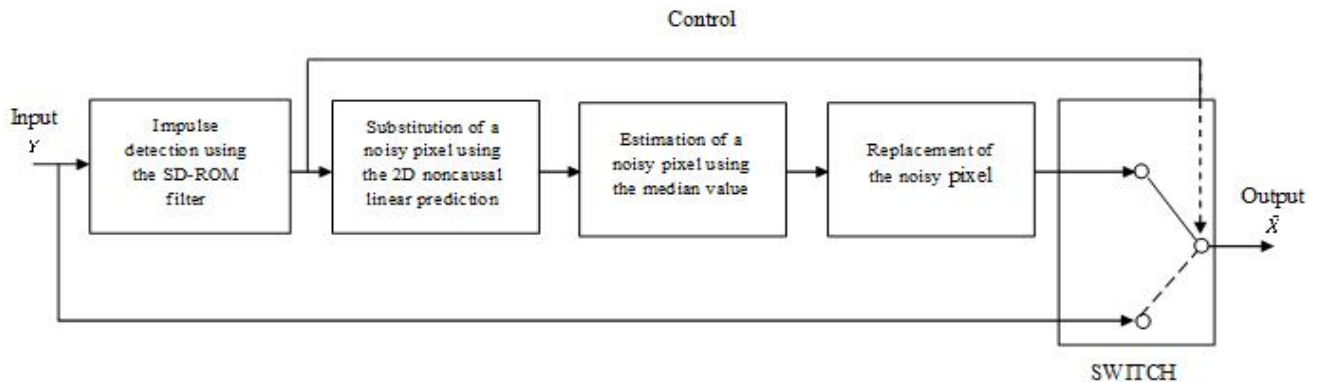


Fig. 1. Block diagram of the proposed switching median filter

V. EXPERIMENTAL RESULTS

A number of experiments are carried out to evaluate the performance of the proposed algorithm with standard grayscale test images having distinct features. The test images are “Lena” (512×512), “Barbara” (512×512), “Boat” (512×512) and “Cameraman” (256×256). All these images are artificially corrupted with the salt and pepper noise at different noise ratios varying from 10% to 80%. Noisy pixels are detected by the SD-ROM filter. It is implemented by considering a window. The four thresholds selected for the SD-ROM filter are from the following set of values: $= \{4, 8, \text{and } 12\}$, $= \{15, 20\}$, $= 20$, and $= 30$ when the noise density value is below 40% and for higher noise densities (i.e. above 40%); we chose the thresholds to be similar to that appeared in [5].

In the first set of our experiments, we evaluate the performance of the impulse noise detection method that we have used in this paper. Table I presents PSNR performance of the proposed method with two impulse detection methods, namely, the detection of extreme values of brightness (i.e. 0 and 255) (DEVB) as reported in the NSW filter, and that of the SD-ROM filter, on the “Lena” image corrupted by salt and pepper noise at various levels. The results indicate that the proposed method with SD-ROM detection performs better than the detection method used by the NSW filter in terms of PSNR. On the other hand, Table II shows the number of missed detections and the number of false detections against noise corruptions at different densities by using the SDROM detection.

In the next set of our experiments, we study the efficacy of the noncausal linear prediction methods. To do this, first we consider the first-order 2D noncausal linear prediction on a 3×3 neighborhood window around the center pixel. Considering its position as (0, 0) in the window, the prediction coefficients are computed by Equation (5). Finally, the center pixel is estimated by Equation (4). Next, we have carried out experiments using the second-order 2D noncausal linear prediction that utilizes the 8-neighborhood pixels in a 3×3 window. In this case, the center value is estimated by using Equation (7). It may be mentioned here that for low noise densities, the second-order noncausal prediction leads to slight improvement in the final filtering result over the first-order noncausal linear prediction in terms of the peak signal-to-noise ratio (PSNR). However, at high noise densities (i.e. above 40%), the PSNR improves significantly over that obtained with the first-order prediction. The improvement is clearly due to the inclusion of the diagonal neighbors along with the 4-neighbors in the second-order prediction. Detail results are presented in Table-III for the “Lena” image corrupted by salt and pepper noise at varying densities. The only limitation that we observed in the case of second-order prediction is due to the increase in the overall computational complexity. The time required to run the proposed algorithm at high noise densities is significantly higher than the one

using the first-order prediction. We have also seen that the proposed algorithm with second-order prediction fails to give better performance than the NSW filter method at high noise densities. Therefore, in order to evaluate the performance of the proposed switching median filter at low to medium noise densities and to minimize the overall computational complexity, we mainly concentrate on the first-order 2D noncausal linear prediction for the rest of our experiments.

Finally, we have compared the filtering performance of the proposed scheme with other switching based median filters including the SD-ROM, the ACWM, the DWM, the ASWM, and the NSW filters in terms of the mean-square error (MSE) and the peak signal-to-noise ratio (PSNR). Table IV shows the comparison of output PSNR and MSE values for different filters for the “Lena” image at different percentages of salt and pepper noise. Similarly, Table V shows the corresponding results for the “Boat” image. The results clearly indicate that the proposed filter outperforms the state-of-the-art in terms of PSNR and MSE values for both the test images when corrupted by the salt and pepper noise up to 40%. It is observed that the performance of the proposed method deteriorates for noise densities above this value as compared to that of the NSW filter. This is because at higher noise densities the probability of getting more than one impulse within the 2D neighborhood window becomes higher, leading to poor prediction of the center pixel, whereas in the NSW filter, the prediction of the center pixel is done from the noise free pixels in a sorted 1D array. However, the results show that the proposed filter outperforms the SD-ROM filter, the DWM filter, and the ASWM filter even at noise ratios beyond 60%.

Fig. 2(b)-2(g) show the outputs of various filtering methods for the “Lena” image when 40% of the total pixels are corrupted by the salt and pepper noise. From a visual inspection of the output images, it is observed that the proposed filter not only able to remove the noise but also successfully preserves the detail features in the image. Similarly, Fig. 4(b)-4(g) show the results for the “Barbara” image when corrupted by 50% salt and pepper noise. As expected, it is observed that the visual quality of the output of the proposed filter degrades as the noise ratio is increased to 50% or more. The performances of the proposed method and other considered filters for “Cameraman” image corrupted by salt and pepper noise at different levels in terms of PSNR and MSE are reported in Fig.3. The results show that the proposed method clearly performs better than other methods up to 40-45% of noise in terms of both the parameters.

CONCLUSIONS

An improved switching based median filter has been proposed based on the concept of substitution, prior to estimation for the removal of salt and pepper noise from gray scale images. The algorithm consists of two stages. In the first stage, the impulses are detected by the impulse detection mechanism of the SD-ROM filter. In the second stage, the noisy pixel is first predicted using the 2D non causal linear

prediction technique and subsequently it is replaced by the median of its neighborhood pixels. The experimental results show that the proposed filter performs better than other schemes like the SD-ROM, the ACWM, the DWM, the ASWM, and the NSWAM filters both visually and quantitatively up to medium level of impulse noise corruption. However, at high noise levels NSWAM filter outperforms the proposed filter. The NSWAM filter is based on first order causal linear prediction only, and does not consider the 2D correlation of the image pixels. Therefore, it results in blurring of the detail features in the image at low to medium noise levels as opposed to the proposed filtering scheme. Work is currently in progress to extend the proposed method for the removal of random valued impulse noise.

TABLE I. PERFORMANCE COMPARISON OF THE PROPOSED FILTER WITH DIFFERENT IMPULSE NOISE DETECTION METHODS

Method	% of Noise					
	10	20	30	40	50	60
DEVB	41.93	37.68	34.30	30.80	27.48	23.88
SD-ROM	42.17	37.96	34.73	31.53	28.76	24.94

TABLE II. PERFORMANCE ANALYSIS OF THE SDROM DETECTION METHOD AT DIFFERENT NOISE DENSITIES

% of Noise	Missed Detection	False Detection
10	43	440
20	252	474
30	914	566
40	2300	637
50	5886	925
60	11723	1456

TABLE III. RESULTS OF THE PROPOSED FILTER WITH DIFFERENT ORDERS OF PREDICTION ON "LENA" IMAGE AT DIFFERENT NOISE DENSITIES

Proposed Method Using	% of Noise						
	20	30	40	50	60	70	80
First-order Prediction	37.96	34.73	31.53	28.76	24.94	17.58	13.98
Second-order Prediction	37.98	34.76	31.94	29.44	26.06	21.89	17.16

TABLE IV. PERFORMANCES OF VARIOUS FILTERS ON "LENA" IMAGE AT DIFFERENT NOISE DENSITIES. (A) PSNR IN DB AND (B) MSE

Method	% of Noise					
	10	20	30	40	50	60
SD-ROM[5]	32.98	31.45	29.32	27.02	23.93	20.16
ACWM[7]	39.93	35.57	31.68	28.13	23.99	20.32
DWM[8]	39.94	36.16	33.32	31.44	28.86	25.45
ASWM[9]	33.27	32.78	31.06	29.21	25.51	20.69
NSWM[10]	41.52	37.23	34.30	31.24	30.52	28.44
Proposed	42.08	37.96	34.73	31.53	28.76	24.94

(B)

Method	% of Noise					
	10	20	30	40	50	60
SD-ROM[5]	32.69	46.50	76.04	131.13	272.96	625.75
ACWM[7]	6.59	18.02	44.13	99.91	259.25	603.69
DWM[8]	6.50	16.33	36.04	54.75	88.28	213.31
ASWM[9]	30.04	35.73	50.86	77.91	182.62	554.12
NSWM[10]	4.21	11.17	20.81	38.78	57.64	92.99
Proposed	3.39	8.53	18.82	37.98	90.96	224.90

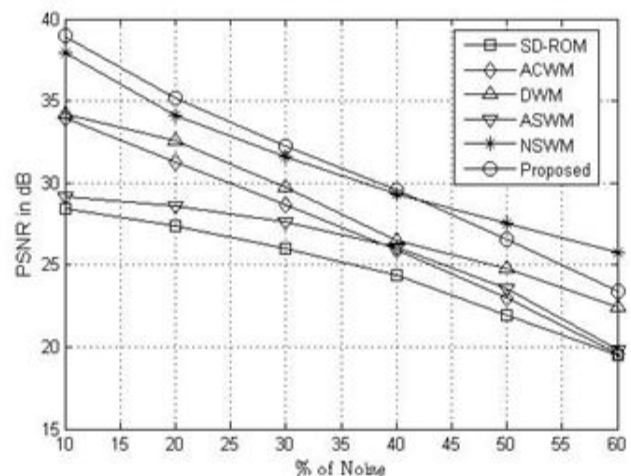
TABLE V. PERFORMANCES OF VARIOUS FILTERS ON "BOAT" IMAGE AT DIFFERENT NOISE DENSITIES. (A) PSNR IN DB AND (B) MSE

(A)

Method	% of Noise					
	10	20	30	40	50	60
SD-ROM[5]	28.43	27.39	26.01	24.36	21.97	19.48
ACWM[7]	33.99	31.26	28.65	25.89	22.99	19.58
DWM[8]	34.21	32.60	29.70	26.48	24.81	22.39
ASWM[9]	29.13	28.63	27.60	26.08	23.60	19.80
NSWM[10]	37.96	34.12	31.58	29.33	27.51	25.72
Proposed	38.96	35.16	32.26	29.58	26.60	23.37

(B)

Method	% of Noise					
	10	20	30	40	50	60
SD-ROM[5]	93.14	118.50	163.26	237.94	412.85	732.64
ACWM[7]	25.90	48.63	88.52	167.23	326.14	715.70
DWM[8]	22.04	39.69	60.28	146.18	214.54	374.61
ASWM[9]	79.43	91.24	112.79	160.04	283.30	679.61
NSWM[10]	10.18	25.77	45.19	75.72	115.33	174.03
Proposed	8.26	19.82	38.65	71.62	142.37	298.99



(a)

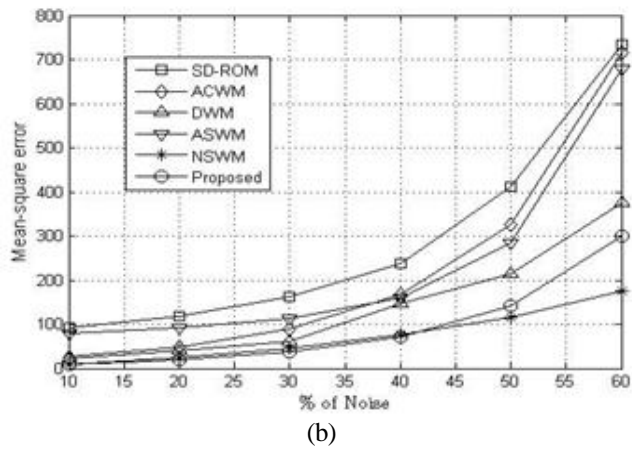


Fig. 3. Performance comparison of different methods for filtering "Cameraman" image degraded by various levels of salt and pepper noise. (a) PSNR vs. % of Noise. (b) MSE vs. % of Noise.

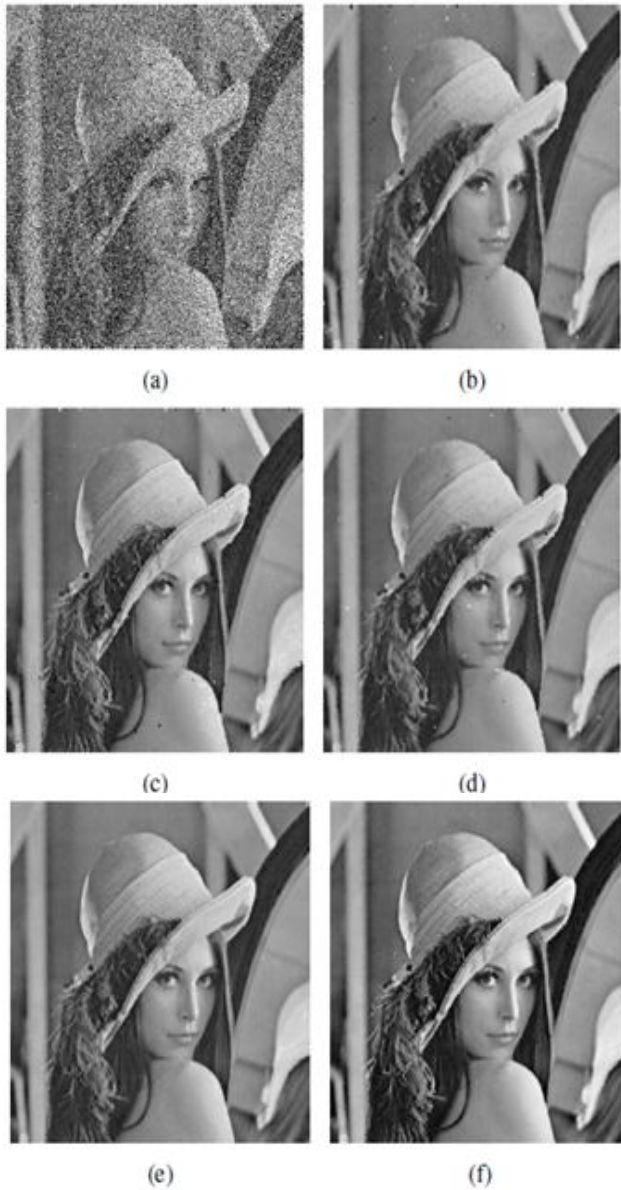


Fig. 2. Performance of different filters for "Lena" image with 40% salt and pepper noise. (a) Noisy. (b) SD-ROM. (c) ACWM. (d) ASWM. (e) DWM. (f) NSWM. (g) Proposed and (h) Original.



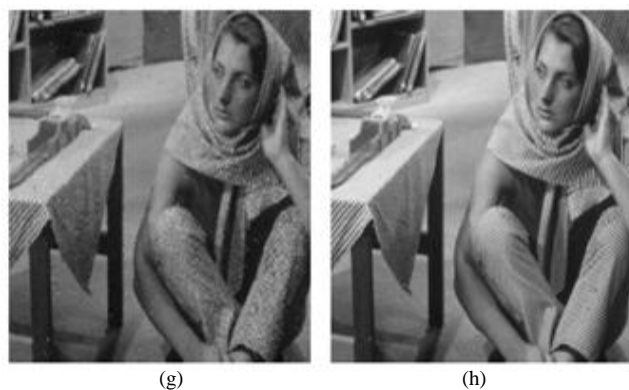


Fig. 4. Performance of different filters for “Barbara” image with 50% salt and pepper noise. (a) Noisy. (b) SD-ROM. (c) ACWM. (d) ASWM. (e) DWM. (f) NSWM. (g) Proposed and (h) Original.

REFERENCES

- [1] W. Pratt, *Digital Image Processing*. John Wiley & Sons Inc, 1978.
- [2] R. K. Brownrigg, “The weighted median filter,” *Commun. ACM*, vol. 27, pp. 807–818, August 1984.
- [3] S.-J. Ko and Y. Lee, “Center weighted median filters and their applications to image enhancement,” *IEEE Transactions on Circuits and Systems*, vol. 38, no. 9, pp. 984–993, September 1991.
- [4] R. C. Hardie and K. E. Barner, “Rank-conditioned rank selection filters for signal restoration,” *IEEE Transactions on Image Processing*, vol. 2, pp. 192–206, 1994.
- [5] E. Abreu and S. Mitra, “A signal-dependent rank ordered mean (SDROM) filter—a new approach for removal of impulses from highly corrupted images,” in *ICASSP*, vol. 4, pp. 2371–2374, 1995.
- [6] T. Chen, K. K. Ma, and L. H. Chen, “Tri-state median filter for image denoising,” *IEEE Transactions on Image Processing*, vol. 8, no. 12, pp. 1834–1838, Dec. 1999.
- [7] T. Chen and H. R. Wu, “Adaptive impulse detection using center weighted median filters,” *IEEE Signal Processing Letters*, vol. 8, no. 1, pp. 1–3, January 2001.
- [8] Y. Dong and S. Xu, “A new directional weighted median filter for removal of random-valued impulse noise,” *IEEE Signal Processing Letters*, vol. 14, no. 3, pp. 193–196, March 2007.
- [9] S. Akkoul, R. Ledee, R. Leconge, and R. Harba, “A new adaptive switching median filter,” *IEEE Signal processing Letters*, vol. 17, pp. 587–590, June 2010.
- [10] V. Jayaraj and D. Ebenezer, “A new switching-based median filtering scheme and algorithm for removal of high-density salt and pepper noise in images,” *EURASIP Journal on Advances in Signal Processing*, vol. 2010, pp. 50:1–50:11, 2010.
- [11] A. Asif and J. M. F. Moura, “Image codec by noncausal prediction, residual mean removal, and cascaded VQ,” *IEEE Transactions on Circuits and Systems for Video Technology*, vol. 6, pp. 42–55, 1996.
- [12] S. Haykin, *Adaptive filter theory (3rd ed.)*. Upper Saddle River, NJ, USA: Prentice-Hall, Inc., 1996.
- [13] A. Jain, *Fundamentals of Digital Image Processing*. Prentice Hall, 1989.